IEEE Access
Multidisciplinary | Rapid Review | Open Access Journal

Received 20 December 2023, accepted 11 January 2024, date of publication 17 January 2024, date of current version 25 January 2024.

Digital Object Identifier 10.1109/ACCESS.2024.3355191

RESEARCH ARTICLE

Assessment of Exposure to Spatially Varying Magnetic Fields in MRI Environments: Modeling Analysis for Simulation Tools

VALENTINA HARTWIG[1], MARIANNA CIANFAGLIONE[2], FRANCESCO CAMPANELLA[3], MARIA ANTONIETTA D'AVANZO[3], CARLO SANSOTTA[4], AND GIUSEPPE ACRI[4]

[1]CNR, Institute of Clinical Physiology, 56124 Pisa, Italy
[2]Scuola di Ingegneria, Università di Pisa, 56124 Pisa, Italy
[3]Sezione di Supporto Tecnico al SSN in Materia di Radiazioni dell'INAIL, Istituto Nazionale Infortuni sul Lavoro (INAIL), 00144 Rome, Italy
[4]Dipartimento di Scienze Biomediche, Odontoiatriche e Delle Immagini Morfologiche e Funzionali, Università Degli Studi di Messina, 98125 Messina, Italy

Corresponding author: Valentina Hartwig (valentina.hartwig@cnr.it)

This work was supported by Istituto Nazionale Infortuni sul lavoro (INAIL) within the programme Bando ricerche in collaborazione (BRIC)-2022— ID55 Project CUP: J43C22001390005.

ABSTRACT Magnetic resonance imaging (MRI) is a non-invasive diagnostic technique widely used in medicine with more than 60 million exams per year performed worldwide. MRI personnel are always exposed to static and spatially heterogeneous magnetic fields (fringe or stray fields) and motion-induced time-varying magnetic fields during the working day. This kind of exposure can evoke vertigo and other sensory perceptions such as nausea, visual sensations, and a metallic taste which are not considered hazardous per se, but can be disturbing and may impair working ability. Up to now, no standardized procedures have been available in the literature for the assessment of occupational exposure in an MRI environment. The goal of this paper is to give some indications about the analytical models underlying the development of digital tools for occupational exposure assessment in MRI environments, to have easy but interactive educational tools, for educating MRI staff to avoid higher-risk conditions, and to draw up the best practices. Analysis of the models for the estimation of the magnetic field spatial distribution and the representation of the workers' movements is described and finally, some recommendations for an accurate methodology to use in simulation tools for exposure assessment are given.

INDEX TERMS MRI safety, occupational exposure, static magnetic field, time-varying magnetic field, induced electric field, human movements.

I. INTRODUCTION

Magnetic resonance imaging (MRI) is a non-invasive diagnostic technique widely used in medicine with about 50,000 MRI machines worldwide. Nowadays it is estimated that more than 60 million exams per year are performed worldwide [1].

MRI does not pose ionizing radiation risk but, mainly because of the rapid development of MR technologies, possible health hazards have recently gained increased attention. Specifically, MRI personnel are always exposed to static and spatially heterogeneous magnetic fields (fringe or stray fields) during the working day [2], [3]. Also, moving around the MR room to perform their functions, technicians and other workers are exposed to a slowly time-varying magnetic field, that induces electrical currents and fields in the body. This exposure leads to the onset of transient symptoms. Dizziness, vertigo, visual disturbances, nystagmus, and metallic taste were the most frequently reported symptoms induced by worker movements in the fringe field [4]. Many studies highlighted the occurrence of transient symptoms, often defined as sensory effects [5], [6], [7], [8].

In the last few decades, studies have been published regarding the long-term biological effects of static magnetic fields; however, the results are often contradictory and confusing. Some studies on genotoxic or carcinogenic effects have been

The associate editor coordinating the review of this manuscript and approving it for publication was Lei Zhao.

conducted [9], [10], [11], but the available evidence is not sufficient to draw firm conclusions. Only a few epidemiological studies have been conducted [11] addressing the effects of magnetic field exposure in terms of cancer risk but they lack accuracy. Effects on cardiovascular function, including arterial blood pressure and peripheral blood flow, are less clear [12]. In general, chronic and long-term effects due to exposure to magnetic fields have been reported in only a few studies [13], [14].

International Commission on Non-Ionizing Radiation Protection published several guidelines that set exposure limits [15], [16], [17], [18] and include them to those imposed by the Directive [19], [20], [21] issued by the European Parliament and the Council of the European Union.

In particular, the ICNIRP guidelines [15] show that the movement-induced electric field can evoke vertigo and other sensory perceptions such as nausea, visual sensations (known as magnetophosphenes), and a metallic taste if the field intensity is high enough. There is also the possibility of acute neurocognitive effects with subtle changes in attention, concentration, and visuospatial orientation [22], [23], [24]. These effects are not considered hazardous per se, but they can be disturbing and may impair working ability. By following ICNIRP and European regulations, MRI workers should receive all necessary information about the outcome of the risk assessment, including preventive measures taken to minimize exposure, and they should be trained about the possibility of transient symptoms and sensations, and how to detect and report adverse effects of such exposure. A good and detailed training should also include the complete knowledge of the specific exposure conditions.

For example, the identification of the area in which the magnetic spatial field gradient is maximal is a crucial point [25]. Moreover, a classification of the categories and/or procedures for which exposure to motion-induced time-varying magnetic fields is highest could be very important to provide complete information and best practices for the workers [26].

Many studies can be found in the literature regarding the assessment of MRI staff exposure to static magnetic fields and slowly time-varying magnetic fields owing to the movement in a spatially heterogeneous magnetic field [27], [28], [29], [30], [31], [32], [33], [34], [35]. Most of these studies were based on theoretical models or personal measurements of exposure to magnetic fields, using dosimeters. For example, in [27] and [28], Hartwig and colleagues presented, for the first time, a digital tool to simulate the linear path followed by an MRI worker during a routine procedure and calculate the induced electric field: the tool used the spatial distribution of the stray magnetic field obtained by the knowledge of the isogauss line map of a specific MR scanner. A similar tool was then used by Sannino et al. [29] to estimate the motion-induced time-varying electric fields during a study of biomonitoring of MRI staff. On the back of these studies, Gurrera et al. [30] presented an analytical model to verify the compliance of the exposure with the Directive: the model was based on the 3D map of the stray field of a magnetic dipole. Later, they added to the model an accurate human movements analysis: full body motion was recorded in a gait laboratory arranged to reproduce the workspace of a room with an MRI full-body scanner, by using a stereophotogrammetric system to obtain speed trend during the movements [31]. Commercial personal dosimeters were instead used by Acri et al. [32] to measure the magnetic flux density related to the operator movement inside the MRI room and then calculate the corresponding dB/dt curves. The dB/dt peak values have been compared with the reference level (RL) proposed by ICNIRP. Similar measurements were carried out later [33] in different MRI facilities for two classes of MRI workers concluding that the RL always exceeds during measurements on the 3.0 T scanner and sometimes on 1.5 T. Finally, Belguerras et al. [34] combined an analytical model to estimate the magnetic field exposure during movements, with a vision-based system to detect the person's body parts. In this study, a homemade personal dosimeter [36] was also used to measure the magnetic field at the neck level of the worker and validate the proposed approach.

Regarding the assessment of occupational exposure in an MRI environment, especially when dealing with static magnetic fields and time-varying magnetic fields due to movement, no standardized procedures have been available in the literature up to now.

The purpose of this work is hence to shed light on this issue, starting from the analysis of some mathematical models that are the basis of a rigorous methodology to assess MRI staff exposure. Analysis of the models for the estimation of the magnetic field spatial distribution and the representation of the workers' movements is described. Recommendations for an accurate methodology to use in simulation tools for exposure assessment are finally given.

II. METHODS

A. INDUCED ELECTRIC FIELD CALCULATION

From the electromagnetic field theory, an electric conductor, such as the human body, which moves in spatial heterogeneous static magnetic fields B (fringe field), induces an electrical field E, according to Faraday's law. The induced field can be calculated as suggested in the guidelines of the ICNIRP [15]:

$$E = C(dB/dt) = C(dB/ds)v \tag{1}$$

where *dB/dt* is the time derivative of magnetic flux density, *dB/ds* is the spatial gradient of the magnetic flux density, and *v* is the walking speed of the exposed workers.

C is "a conversion factor that depends on the location within the body, the size of the body, the shape of the body, electrical properties of the tissue as well as on the direction and distribution of the magnetic field" [15]. *C* is measured in [V $m^{-1}Ts^{-1}$] and can be determined by using numerical simulations on a realistic and heterogeneous model of the human body or body region of interest [15].

B. MAGNETIC FLUX DENSITY MODEL

The spatial distribution of the static magnetic field in the area where the workers mainly move during their daily work was estimated starting from the measurement of magnetic flux density |B| using a commercial 20T-Hallprobe Three-axis Hall Magnetometer THM1176 (Metrolab Instruments SA, Switzerland). A total of 432 measurements were performed at two representative heights above the ground (y1=1.15 m and y2=1.6 m) following an 18 × 12 grid on the xz plane (parallel to the ground plane) with a step of 0.10 m. For a 1.70 m tall worker, the chosen heights correspond to the chest and the head respectively. The cover area was the frontal area to the right of the patient's bed ($-1.40 \leq x \leq -0.30$ m, $1.00 \leq z \leq 2.70$ m, $y1 = 1.15$ m, and $y2 = 1.6$ m). The magnetic flux density field value at each point of the area of interest ($-1.40 \leq x \leq 1.40$ m, $1.00 \leq z \leq 2.70$ m, $y1 = 1.15$ m and $y2 = 1.6$ m) was estimated by fitting the measured data using a cubic spline interpolation, to obtain a detailed map (with a resolution of 0.01 m) for each plane. The magnetic flux density map obtained by this model was then compared with the data obtained by isogauss lines (approximated to ellipses) which have been interpolated using first a triangulation-based natural neighbor interpolation (below "natural") and then a piecewise exponential model (below "exponential") [27]. The accuracy of the model was evaluated using the Symmetric Mean Absolute Percentage Error (sMAPE) [34] calculated between simulated B_{est} and measured B_{meas} data as follows:

$$\bar{\varepsilon} = \frac{1}{N} \sum_{N}^{i=1} 100 \cdot (2 \cdot |B^i_{meas} - B^i_{est}| / |B^i_{meas} + B^i_{est}|) \quad (2)$$

where N is the total number of |B| values.

Moreover, the relative error between simulated and measured data was calculated for each point of measurement and shown as a heatmap. Correlation between estimated and measured |B| values was also evaluated using Pearson's correlation coefficient R.

C. HUMAN BODY MODEL

For the calculation of the induced electric field, we considered a human body model standing in the MRI environment. The body of a generic operator moving within the MRI room was modelled by a rigid body that rotates and translates in a three-dimensional space. The rigid body consisted of three elliptical closed loops, two for limbs and one for the trunk, while a circular loop was chosen to model the head. The dimensions of all parts of the body were defined according to the anthropometric tables [37] which contain data on human body size and shape and are the basis upon which all digital human models are constructed. In these tables, all the measurements are derived as a proportion of the height.

With this representation of the human body, the conversion factor C was calculated using the following equation for the head (Equation 2) and for the trunk (Equation 3) [38]:

$$C = r/2 \quad [\mathrm{Vm^{-1}Ts^{-1}}] \quad (3)$$

considering a circular loop with radius r for the head, and

$$C = (a^2 b)/(a^2 + b^2) \quad [\mathrm{Vm^{-1}Ts^{-1}}] \quad (4)$$

considering elliptical loops for the trunk, where a is the semi-length of the major axis, and b is the semi-length of the minor axis of each ellipse. In our model, the major axis 2^*a of the ellipse is equal to the length of the trunk, while the minor axis 2^*b of the ellipse is the width. The radius of circular loop r is the radius of the model's head. These parameters were calculated using the anthropometric tables starting from the knowledge of the worker's height and sex. For using the conversion factor, the component of the magnetic flux density must be normal to the loop surface.

D. TRANSLATION AND ROTATION MOVEMENTS

Besides of the translation movements, we also considered the rotation of the human model with respect to the vertical axes y. Specifically, two rotation joints have been added to the model to simulate the relative rotation of the trunk with respect to the floor and the relative rotation of the head with respect to the trunk. To describe the movements of the rigid body in the three-dimensional space we considered the global reference system positioned at the isocenter of the MRI scanner and the local reference system of the rigid body positioned at the foot of the human body model. Both reference systems had the x, y, and z-axis directed as specified by the isogauss lines map given by the MRI scanner manufacturer. As reference configuration, the operator was positioned at the MRI room door location, so the local reference system was shifted from the global reference system considering the size of the MRI room.

To describe the rigid body motion in space, Euclidean transformations have been used, to preserve the Euclidean distance between every pair of points in the model [39]. Any rigid transformation was decomposed in a rotation followed by a translation. The operator's final position after his movement is described by homogeneous matrices.

E. MOVEMENT SPEED MODEL

A theoretical model of the operator movements was created by combining rotation and translation motions. In particular, it has been considered a circular motion of an infinitesimal element placed at the end of the minor axis of the elliptical loop, for each limb, or at the end of the radius of the circular loop, for the head. Each element had a speed given by the sum of the speed of linear translation applied to the center of gravity and the speed due to the rotation around the axis passing through its center of gravity and perpendicular to the floor. An inverted pendulum model has been applied for the translational movement of each leg: during the support phase, the center of mass of the model runs an arc trajectory of a circle of radius equal to the length of the leg. To travel this trajectory, the centre of mass needs a centripetal force, depending on body speed. By these considerations, the maximum walking speed v_{max} was obtained as follows:

$$v_{max} = \sqrt{Lg} \quad (5)$$

where L is the length of the leg (obtained from the anthropometric tables) and g is the acceleration of gravity.

For example, choosing a height of 1.70 m, L is equal to about 0.90 m, and hence the v_{max} results of about 3 m/s.

For the rotational component of the movement, an angular speed was calculated considering the rotation angle θ and the time. The final speed was equal to:

$$v_{trasl} + v_{rot} = v_{trasl} + rd\theta/dt \tag{6}$$

where r is the distance between the infinitesimal element and the rotation axes.

A dynamic speed model, which results in a trapezoidal profile, can be chosen so the maximum value is reached when the user has finished the rotation. The path has been divided into three sections on which the following equations have been applied to obtain the required profile. The speed model considers an initial accelerated motion, followed by a constant motion and then a decelerated motion.

The selected maximum translation speed is 1 m/s to which the rotational speed has been added. For the deceleration section, it was assumed that the user decelerates with the same acceleration.

Regarding the only rotational movements, such as the rotation of the head with the feet fixed at the same point, we considered a worker standing near the patient bed with the shoulders facing the patient which rotates the head 90° from the panel placed on the gantry side to the patient. The rotation speed was chosen as 180°/s. In this case, we considered the magnetic flux density field map at y2 = 1.6 m, corresponding to the head height from the ground for a worker 1.70 m tall.

F. TEST SCENARIO

For the validation of the simulation tool, we need some scenarios that should approximate real situations. One of the most suitable methodologies is using digital video cameras to record the movements of operators during their routine work. For research purposes, it is also possible to use a camera stereophotogrammetric system and related processing software opportunely arranged. All these solutions can obtain the essential information to be passed to the model, i.e. translation speed, linear trajectory, and points of change of direction.

Using a digital video camera placed in front of the window of the MRI console room, we captured a video during the patient preparation for standard clinical MRI exams.

Then, the video was analyzed by using video processing software (VirtualDub 1.10.4) to obtain the trajectory to reproduce in the simulation tool (walking path characteristics as starting/finish points, direction, position…). For this scenario, we calculated the exposure parameters, in terms of |dB/dt| and |E|, and the speed trend corresponding to the specific analysed movements.

All the calculations have been performed using a homemade dedicated software and its updating [27], [28].

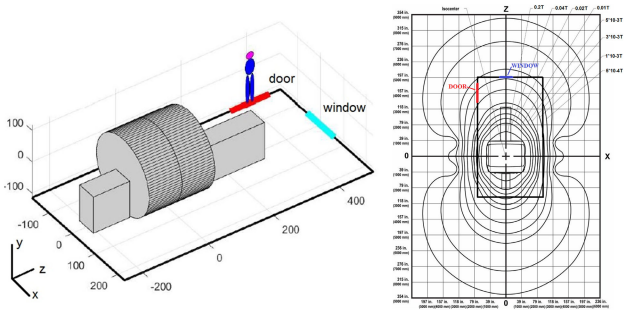

FIGURE 1. 3D representation of the MRI scanner (left) and ground plan representation of the isogauss lines (unperturbed magnetic flux density) (right).

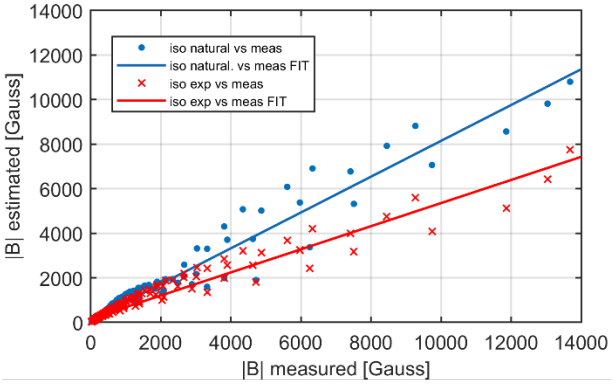

FIGURE 2. Comparison of |B| data estimated by isogauss lines (using two different models) and measured.

III. RESULTS

First of all, a detailed 3D map of the specific MR room was obtained using both graphical maps and physical measurements. Figure 1 shows the 3D representation of the MR scanner inside the dedicated facility (GE_Signa_HD 3T at Fondazione Toscana G. Monasterio, Italy) as well as was reproduced inside the simulation tool. The 3D map also shows the human body model placed at the room door location.

Figure 1 also shows (on the right) the ground plan representation of the unperturbed magnetic flux density using isogauss lines, as provided by the manufacturer, relative to the scanner isocentre quote from the ground (@1.15 m).

Figure 2 shows the comparison of |B| data estimated by isogauss lines (using two different models) and measured. Results of linear fitting are shown for the triangulation-based natural neighbor interpolation (iso natural) and the piecewise exponential model (iso exp).

Table 1 reports the minimum (err_{min}) and maximum (err_{max}) relative error values for both the interpolation methods with respect to the measured data, the value of sMAPE ($\bar{\varepsilon}$), and the correlation coefficient R together with the p-value.

According to these results, the triangulation-based natural neighbor interpolation was more accurate compared to the piecewise exponential model for the |B| mapping. Figure 3 reports the heatmap of the relative error between simulated

TABLE 1. Results of comparison between B field mapping methods.

Method	err_{min}	err_{max}	$\bar{\varepsilon}$	R	p
iso natural vs measured	0.13	59.78	13.53	0.98	<0.001
iso exponential vs measured	0.10	61.59	14.75	0.97	<0.001

data, calculated with triangulation-based natural neighbor interpolation, and measured data for each point of measurement.

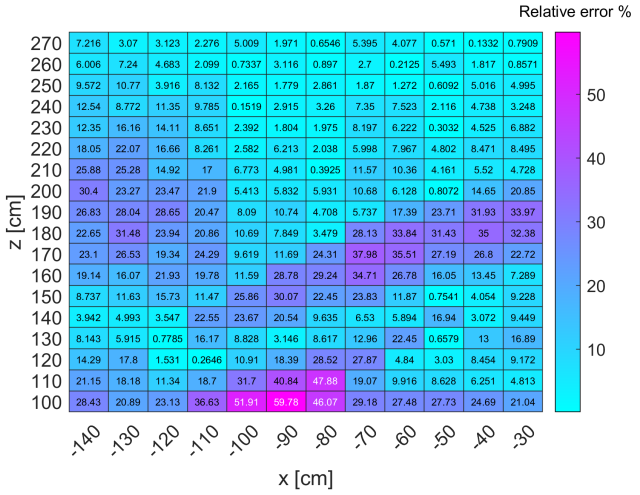

FIGURE 3. Heatmap of the relative error between simulated data, (triangulation-based natural neighbor interpolation) and measured data.

Figure 4 shows the coloured scale map of the magnetic flux density in the area where the workers mainly move during their daily work, calculated from the measurements (represented with circles in the figure) using cubic spline interpolation, for the xz plane parallel to the ground (@1.15 m). The magnetic flux density spatial distribution was used in the simulation tool to calculate the |B| values along the simulated trajectory of the test scenario and then all the other exposure parameters, i.e. induced electric field and magnetic field changes over time.

Figure 5 shows some frames extracted from the video acquired during the test procedure (a radiology technician performing the patient preparation for a brain MRI examination): enters the scanner room (AB), reaches the gantry (BC), moves away from the gantry (CD), exits the scanner room (DE).

In Figure 6, the results for the chosen test scenario are shown together with the representation of the walking path in the MRI scanner room divided into four parts (AB-BC-CD-DE). The graph on the right shows the |B|, |E| and v values along the specified paths (x-axis is relative to the linear movements in the room expressed in meters). Calculated parameters for the test scenario are reported in Table 2: for each path section the maximum value of |B|, |E|, and v is shown. The last column reports the maximum value of |E| calculated using a constant speed model v_{cost} with 1 m/s as the nominal value, instead of the dynamic speed model described in the specific method section.

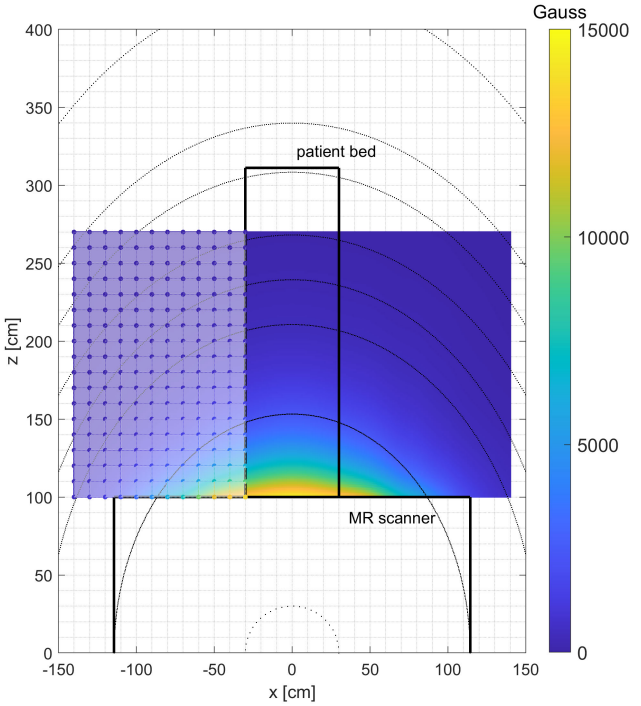

FIGURE 4. Magnetic flux density calculated from the measurement (cubic spline interpolation); xz plane @y =1.15 m.

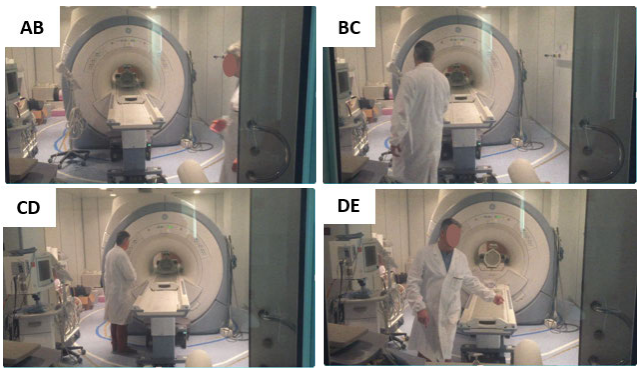

FIGURE 5. Frames extracted from the video acquired during the test procedure.

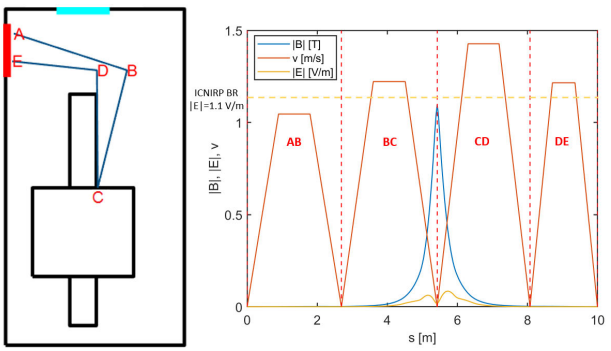

FIGURE 6. Results for the test scenario: representation of the walking path (left); |B|, |E| and v values along the specified paths (right). ICNIRP Basic restriction for controlled exposure conditions is also shown (|E| = 1.1 mV).

TABLE 2. Calculated parameters for test scenario.

Path	$\|B\|_{max}$ (T)	$\|E\|_{max}$ (mV/m)	v_{max} (m/s)	$\|E\|_{max}$ @ v_{cost}=1 m/s (mV/m)
AB	0.0016	0.12	1.05	0.95
BC	1.16	67.00	1.22	312.37
CD	1.16	86.82	1.43	330.45
DE	0.0022	0.26	1.22	18.52

Regarding the head rotation movement, Figure 7 shows the results for the exposure parameters in the specific case of a worker standing close to the gantry (x=35 cm, z=105 cm), with the shoulders facing the patient bed, which rotates the head of 90° from the gantry to the patient.

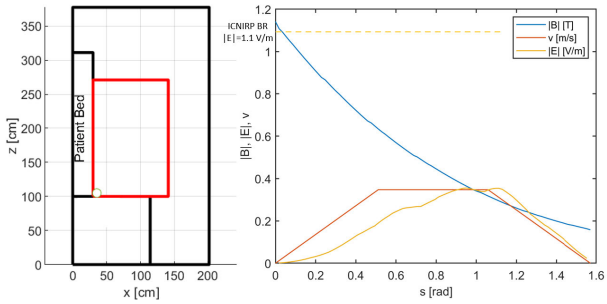

FIGURE 7. Results for the head rotation movement in the proximity of the gantry. ICNIRP Basic restriction for controlled exposure conditions is also shown (|E| = 1.1 mV).

Table 3 shows the results for the head rotation movements considering different positions of the worker in the proximity of the scanner. The last column reports the maximum value of |E| calculated using a constant rotation speed of $\omega_{cost} = 180°/s$ as the nominal value.

TABLE 3. Calculated parameters for head rotation @ ω = 180°/s.

Head Placement	$\|B\|_{max}$ (T)	$\|E\|_{max}$ (mV/m)	v_{max} (m/s)	$\|E\|_{max}$ @ ω_{cost}=180°/s (mV/m)
x=35 cm z=105 cm	1.13	319.59	0.35	413.65
x=50 cm z=105 cm	1.08	28.02	0.35	49.75
x=50 cm z=150 cm	0.17	2.36	0.35	6.58

IV. DISCUSSION

The exposure assessment to the time-varying magnetic field due to the movements of the workers in the MRI scanner room is of particular importance mainly to avoid transient symptoms such as dizziness, vertigo, visual disturbances, nystagmus, and metallic taste. Symptoms such as these, even if they do not pose a health risk, can affect the proper performance of work, especially in emergencies. For this reason, it is necessary to have a simple tool to evaluate the exposure in specific facilities and under specific conditions, mainly to teach the MRI staff the best practices.

Some digital tools are found in the literature mainly based on mapping the stray field in the MRI room and simulating the movements of the workers. For the reconstruction of the magnetic field spatial distribution, isogauss line provided by the scanner manufacturers can be used, but these generally do not cover the entire distribution of the magnetic fields near magnets, and hence they permit only obtaining an approximate method for the evaluation of workers' exposure [27], [28]. The two models based on isogauss lines analysed here, seem both adherent to the measured values (Pearson's coefficient > 0.97) with a sMAPE $<15\%$. Despite this, our results show that |B| values, obtained by the two different interpolation methods from isogauss lines, in some positions, are very different if compared with the values obtained by measurements. The interpolation of the isogauss lines leads to a relative error up to 61.59% with respect to the |B| measured values, right in the operating area in proximity of the gantry, where the |B| value and its spatial gradient are higher. Hence, the presented results show taking |B| measurement over a non-dense grid and using a cubic spline interpolation, permits to obtain a more accurate map of the stray field. This can be made for different quotes from the ground.

Regarding the simulation of human movements in the MRI scanner room, a rigorous and detailed reproduction should involve a careful analysis of the behavioural aspects of staff operating in an MRI environment. Specifically, particular attention should be paid when the MRI operator moves close to the bore for the patient assistance or positioning of coils, but also for the machine setting. In the most simple model, the MRI workers can be supposed to move translationally and with constant speed [27], [28], [30]. To obtain a more rigorous model, it would be necessary to have a full body kinematic characterization of real MRI operators at work, obtained by human movement analysis (HMA) using stereophotogrammetry, an established technique that allows for accurate 3D tracking in the space of the body segments during the execution of locomotion tasks [31]. This gait analysis requires a specific laboratory and instrumentation which are not generally available in MRI facilities. So, a simple speed model can be used: our results show here that using a constant-speed model leads to an overestimation of the induced electric field, both for linear and rotation movements, with respect to using a dynamic speed model (acceleration-constant-deceleration) that better simulates the human gait [40].

In our opinion, using digital video cameras, placed externally to the MRI scanner room, for recording the actual movements of the workers during daily work it is very useful to create a sort of case history of procedures to reproduce with simulation tools. This kind of setup does not require specific and expensive instruments but can be a simple and low-cost means to classify the categories and/or procedures for which exposure to motion-induced time-varying magnetic fields is highest.

Regarding the linear and rotation movements, given the obtained results, we can assert that fast head rotation close to the gantry results in the highest value of induced electric field (see Table 3). However, by changing the head placement, it is very easy to find the lowest exposure conditions. For example, as it is possible to note from Table 3, if the operator

moves only 15 cm away from the bed along the x-axis, the calculated induced electric field is reduced by about 90%.

The results presented here in terms of induced electric field, are valid under the chosen specific exposure conditions and for the chosen modelling parameters. For this reason, a comparison with results reported in similar works [29], [30], [31] is difficult, also since the lack of a standard procedure to estimate the electric fields induced by exposure to time-varying magnetic fields.

Moreover, a rigorous procedure to verify the compliance of the exposure metrics with the imposed limits should include a frequency analysis [28] and the implementation of the weighted peak method (WPM), according to ICNIRP guidelines [15], [17].

V. CONCLUSION

The main scope of this paper is to give some indications about the analytical models underlying the development of digital tools for occupational exposure assessment in MRI environments.

The aim of this approach is not so much the verification of compliance with the imposed safety limits, but rather to have easy but interactive educational tools, for educating MRI staff to avoid higher-risk conditions, and draw up best practices.

In this context, the following tips can be deduced from the analysis carried out in this work:

1. A detailed map of the stray field can be obtained by some measurement of |B| in the MRI room and a cubic spline interpolation model

2. Capturing MRI staff at work can be useful to collect information about procedures and paths, to reproduce actual exposure conditions using digital tools

3. Both translational and rotation movements should be considered. Fast head rotations in proximity to the gantry induce the highest electric field

4. A constant-speed model overestimates the induced electric field value, in comparison to a dynamic-speed model (acceleration-constant-deceleration).

REFERENCES

[1] *Health at a Glance 2023: OECD Indicators*, OECD, Paris, France, 2023.
[2] V. Hartwig, S. Romeo, and O. Zeni, "Occupational exposure to electromagnetic fields in magnetic resonance environment: Basic aspects and review of exposure assessment approaches," *Med. Biol. Eng. Comput.*, vol. 56, no. 4, pp. 531–545, Apr. 2018.
[3] V. Hartwig, G. Virgili, F. E. Mattei, C. Biagini, S. Romeo, O. Zeni, M. R. Scarfì, R. Massa, F. Campanella, L. Landini, F. Gobba, A. Modenese, and G. Giovannetti, "Occupational exposure to electromagnetic fields in magnetic resonance environment: An update on regulation, exposure assessment techniques, health risk evaluation, and surveillance," *Med. Biol. Eng. Comput.*, vol. 60, no. 2, pp. 297–320, Feb. 2022.
[4] G. Bravo, A. Modenese, G. Arcangeli, C. Bertoldi, V. Camisa, G. Corona, S. Giglioli, G. Ligabue, R. Moccaldi, N. Mucci, M. Muscatello, I. Venturelli, L. Vimercati, S. Zaffina, G. Zanotti, and F. Gobba, "Subjective symptoms in magnetic resonance imaging personnel: A multi-center study in Italy," *Frontiers Public Health*, vol. 9, Oct. 2021, Art. no. 699675.
[5] F. de Vocht, E. Batistatou, A. Mölter, H. Kromhout, K. Schaap, M. van Tongeren, S. Crozier, P. Gowland, and S. Keevil, "Transient health symptoms of MRI staff working with 1.5 and 3.0 Tesla scanners in the UK," *Eur. Radiol.*, vol. 25, no. 9, pp. 2718–2726, Sep. 2015.
[6] K. Schaap, Y. Christopher-de Vries, C. K. Mason, F. de Vocht, L. Portengen, and H. Kromhout, "Occupational exposure of healthcare and research staff to static magnetic stray fields from 1.5–7 Tesla MRI scanners is associated with reporting of transient symptoms," *Occupational Environ. Med.*, vol. 71, no. 6, pp. 423–429, Jun. 2014.
[7] K. Schaap, L. Portengen, and H. Kromhout, "Exposure to MRI-related magnetic fields and vertigo in MRI workers," *Occupational Environ. Med.*, vol. 73, no. 3, pp. 161–166, Mar. 2016.
[8] P. C. Rathebe, "Subjective symptoms of SMFs and RF energy, and risk perception among staff working with MR scanners within two public hospitals in south Africa," *Electromagn. Biol. Med.*, vol. 41, no. 2, pp. 152–162, Feb. 2022.
[9] S. Simi, M. Ballardin, M. Casella, D. De Marchi, V. Hartwig, G. Giovannetti, N. Vanello, S. Gabbriellini, L. Landini, and M. Lombardi, "Is the genotoxic effect of magnetic resonance negligible? Low persistence of micronucleus frequency in lymphocytes of individuals after cardiac scan," *Mutation Research/Fundam. Mol. Mech. Mutagenesis*, vol. 645, nos. 1–2, pp. 39–43, Oct. 2008.
[10] S. Ghodbane, A. Lahbib, M. Sakly, and H. Abdelmelek, "Bioeffects of static magnetic fields: Oxidative stress, genotoxic effects, and cancer studies," *BioMed Res. Int.*, vol. 2013, pp. 1–12, Jan. 2013.
[11] *Potential Health Effects of Exposure to Electromagnetic Fields (EMF)*, SCENIHR, Eur. Commission, Luxembourg, U.K., 2015.
[12] V. Hartwig, G. Giovannetti, N. Vanello, M. Lombardi, L. Landini, and S. Simi, "Biological effects and safety in magnetic resonance imaging: A review," *Int. J. Environ. Res. Public Health*, vol. 6, no. 6, pp. 1778–1798, 2009.
[13] S. Bongers, P. Slottje, L. Portengen, and H. Kromhout, "Exposure to static magnetic fields and risk of accidents among a cohort of workers from a medical imaging device manufacturing facility," *Magn. Reson. Med.*, vol. 75, no. 5, pp. 2165–2174, May 2016.
[14] S. Bongers, P. Slottje, and H. Kromhout, "Development of hypertension after long-term exposure to static magnetic fields among workers from a magnetic resonance imaging device manufacturing facility," *Environ. Res.*, vol. 164, pp. 565–573, Jul. 2018.
[15] International Commission on Non-Ionizing Radiation Protection, "Guidelines for limiting exposure to electric fields induced by and by time-varying magnetic fields below 1 Hz," *Health Phys.*, vol. 106, no. 3, pp. 418–425, 2014.
[16] International Commission on Non-Ionizing Radiation Protection, "Guidelines on limits of exposure to static magnetic fields," *Health Phys.*, vol. 96, no. 4, pp. 504–514, 2009.
[17] International Commission on Non-Ionizing Radiation Protection, "Guidelines for limiting exposure to time-varying electric and magnetic fields (1 Hz to 100 kHz)," *Health Phys.*, vol. 99, no. 6, pp. 818–836, 2010.
[18] J. Juutilainen, "Exposure to high frequency electromagnetic fields, biological effects and health consequences (100 kHz-300 GHz)," in *Review of Experimental Studies of RF Biological Effects (100 kHz-300 GHz)*. Oberschleißheim, Germany: ICNIRP, 2009, pp. 90–303.
[19] *Directive 2013/35/EC on the Minimum Health and Safety Requirements Regarding the Exposure of Workers to the Risks Arising From Physical Agents (Electromagnetic Fields)*, European Parliament and Council of the European Union, Luxembourg, U.K., 2013.
[20] *Non-Binding Guide to Good Practice for Implementing Directive 2013/35/EC Volume 2: Case Studies*, European Commission, Luxembourg, U.K., 2015.
[21] *Non-Binding Guide to Good Practice for Implementing Directive 2013/35/EC Electromagnetic Fields Volume 1: Practical Guide*, European Commission, Luxembourg, U.K., 2015.
[22] A. Heinrich, A. Szostek, F. Nees, P. Meyer, W. Semmler, and H. Flor, "Effects of static magnetic fields on cognition, vital signs, and sensory perception: A meta-analysis," *J. Magn. Reson. Imag.*, vol. 34, pp. 758–763, Oct. 2011.
[23] L. E. van Nierop, P. Slottje, M. Van Zandvoort, and H. Kromhout, "Simultaneous exposure to MRI-related static and magnetic fields affects neurocognitive performance: A double-blind randomized crossover study," *Magn. Reson. Med.*, vol. 849, pp. 840–849, Jan. 2015.
[24] L. E. van Nierop, P. Slottje, M. J. E. van Zandvoort, F. de Vocht, and H. Kromhout, "Effects of magnetic stray fields from a 7 Tesla MRI scanner on neurocognition: A double-blind randomised crossover study," *Occupational Environ. Med.*, vol. 69, no. 10, pp. 759–766, Oct. 2012.
[25] V. Hartwig, "Engineering for safety assurance in MRI: Analytical, numerical and experimental dosimetry," *Magn. Reson. Imag.*, vol. 33, no. 5, pp. 681–689, Jun. 2015.

[26] K. H. Mild, J. Hand, M. Hietanen, P. Gowland, J. Karpowicz, S. Keevil, I. Lagroye, E. van Rongen, M. R. Scarfi, and J. Wilen, "Exposure classification of MRI workers in epidemiological studies," *Bioelectromagnetics*, vol. 34, no. 1, pp. 4–81, Jan. 2013.
[27] V. Hartwig, N. Vanello, G. Giovannetti, M. Lombardi, L. Landini, and M. F. Santarelli, "A novel tool for estimation of magnetic resonance occupational exposure to spatially varying magnetic fields," *Magn. Reson. Mater. Phys., Biol. Med.*, vol. 24, no. 6, pp. 323–330, Dec. 2011.
[28] V. Hartwig, N. Vanello, G. Giovannetti, L. Landini, and M. F. Santarelli, "Estimation of occupational exposure to static magnetic fields due to usual movements in magnetic resonance units," *Concepts Magn. Reson. B, Magn. Reson. Eng.*, vol. 44, no. 3, pp. 75–81, Aug. 2014.
[29] A. Sannino, S. Romeo, M. R. Scarfi, R. Massa, R. d'Angelo, A. Petrillo, V. Cerciello, R. Fusco, and O. Zeni, "Exposure assessment and biomonitoring of workers in magnetic resonance environment: An exploratory study," *Frontiers Public Heal.*, vol. 5, p. 344, Dec. 2017.
[30] D. Gurrera, K. K. Gallias, M. Spanò, B. F. Abbate, F. D'Alia, G. Iacoviello, and V. Caputo, "Moving across the static magnetic field of a 1.5 T MRI scanner: Analysing compliance with directive 2013/35/EU," *Phys. Medica*, vol. 57, pp. 238–244, Jul. 2019.
[31] D. Gurrera, A. Leardini, M. Ortolani, S. Durante, V. Caputo, K. K. Gallias, B. F. Abbate, C. Rinaldi, G. Iacoviello, G. Acri, G. Vermiglio, and M. Marrale, "Experimental and modeling analyses of human motion across the static magnetic field of an MRI scanner," *Frontiers Bioengineering Biotechnol.*, vol. 9, May 2021, Art. no. 613616.
[32] G. Acri, B. Testagrossa, and G. Vermiglio, "Personal time-varying magnetic fields evaluation during activities in MRI sites," in *Proc. IFMBE*, vol. 51, 2015, pp. 741–744.
[33] G. Acri, P. Inferrera, L. Denaro, C. Sansotta, E. Ruello, C. Anfuso, F. Salmeri, G. Garreffa, G. Vermiglio, and B. Testagrossa, "DB/DT evaluation in MRI sites: Is ICNIRP threshold limit (for workers) exceeded?" *Int. J. Environ. Res. Public Health*, vol. 15, no. 7, p. 1298, Jun. 2018.
[34] L. Belguerras, A. R. Kadkhodamohammadi, A. Delmas, M. Miralipoor, N. Weber, A. Gangi, J. Felblinger, N. Padoy, and C. Pasquier, "Evaluation of occupational exposure to static magnetic field in MRI sites based on body pose estimation and SMF analytical computation," *Bioelectromagnetics*, vol. 39, no. 7, pp. 503–515, Oct. 2018.
[35] V. Hartwig, C. Sansotta, M. S. Morelli, B. Testagrossa, and G. Acri, "Occupational exposure assessment of the static magnetic field generated by nuclear magnetic resonance spectroscopy: A case study," *Int. J. Environ. Res. Public Health*, vol. 19, no. 13, p. 7674, Jun. 2022.
[36] A. Delmas, N. Weber, J. Piffre, C. Pasquier, J. Felblinger, and P.-A. Vuissoz, "MRI 'exposimetry': How to analyze, compare and represent worker exposure to static magnetic field?" *Radiat. Protection Dosimetry*, vol. 177, no. 4, pp. 415–423, Dec. 2017.
[37] K. Casadei and J. Kiel. *Anthropometric Measurement*. Accessed: Nov. 30, 2023. [Online]. Available: https://www.ncbi.nlm.nih.gov/books/NBK537315/
[38] D. W. McRobbie, "Occupational exposure in MRI," *Br. J. Radiol.*, vol. 85, pp. 293–312, Apr. 2012.
[39] J. M. McCarthy, *Introduction to Theoretical Kinematics*. Cambridge, MA, USA: MIT Press, 1990.
[40] R. Milani, S. Coda, G. Baccani, F. Campanella, M. Mattozzi, and P. Ferrari, "Applicazione del decreto legislativo 159/2016: Valutazione del rischio da movimento nella pratica di risonanza magnetica," INAIL, Rome, Tech. Rep., 2017.

VALENTINA HARTWIG received the degree in electronic engineering (biomedical engineering) from the University of Pisa, in 2003, and the Ph.D. degree in automatics, robotics, and bioengineering from the Engineering Faculty of Pisa, in 2010. Since 2012, she has been a Researcher with IFC-CNR, working on biological effects and safety in magnetic resonance imaging. She is the author of many papers published in peer-reviewed journals, conference proceedings, and book chapters, mainly on modeling and analysis of the interaction between magnetic fields and biological tissues and on exposure assessment methods in MRI environments.

MARIANNA CIANFAGLIONE received the degree in biomedical engineering from the University of Pisa, in 2021. After graduation, she worked in the field of information technology. In 2023, she moved into the healthcare industry. She is currently a Clinical Analyst in the management of hospital digital processes and clinical activities, in both public and private hospitals.

FRANCESCO CAMPANELLA received the degree in physics from the University of Rome "La Sapienza," in 1991. In 1997, he was a Researcher with ISPESL. In 1998, he received the title of qualified expert for second-degree radiation protection. In 2010, he moved to the National Institute for Insurance against Accidents at Work (INAIL). He is the author of many guidelines and good practices in the areas of competence. Since 2016, he has been a member of the Technical Support Section of the National Health Service Regarding Radiation of INAIL.

MARIA ANTONIETTA D'AVANZO received the degree in biomedical engineering from the University of Naples "Federico II," in 2009. She was a Researcher with the Technical Support Section, National Health Service on Radiation of INAIL, INAIL, in 2013. She received the title of CBRN risk expert and the second-degree qualified expert in radiation protection, in 2012 and 2014, respectively. She is the author of guidelines, fact sheets, and monographs in her field of expertise.

CARLO SANSOTTA received the degree in physics (solid state physics) from the University of Messina, in 1989, and the degree in health physics, in 1998. Since 2000, he has been a confirmed full-time Researcher (Adjunct Professor) with the Medicine School, University of Messina. His research interests include applied physics to medicine, biology, environment and architectural heritage, and health physics and information technology applied to the biomedical and healthcare fields.

GIUSEPPE ACRI received the degree in physics from the University of Calabria and the degree in medical physics from the University of Messina. He has been an Associate Professor with the University of Messina. The scientific research activity has developed in the field of health physics and biomedical physics. His research interests include physical-medical applications in MRI diagnostics and developing phantoms and software to conduct quality controls. In recent years, much attention has also been paid to Raman and NIR spectroscopic techniques and their applicability to both human and veterinary medicine.

Open Access funding provided by 'Consiglio Nazionale delle Ricerche-CARI-CARE-ITALY' within the CRUI CARE Agreement